

# Size and Origins of Long-Range Orientational Water Correlations in Dilute Aqueous Salt Solutions

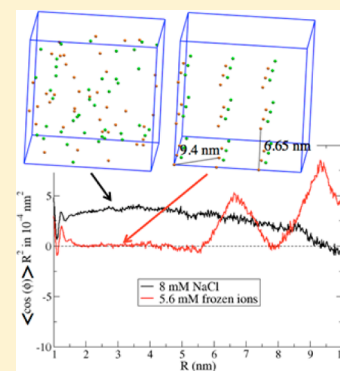
Eva Pluhařová,<sup>\*,†,‡</sup> Damien Laage,<sup>\*,†,§</sup> and Pavel Jungwirth<sup>\*,§</sup>

<sup>†</sup>PASTEUR, Département de chimie, École normale supérieure, PSL Research University, Sorbonne Universités, UPMC Univ. Paris 06, CNRS, 75005 Paris, France

<sup>‡</sup>J. Heyrovský Institute of Physical Chemistry, Czech Academy of Sciences, v.v.i., Dolejškova 3, Prague 18223, Czech Republic

<sup>§</sup>Institute of Organic Chemistry and Biochemistry, Czech Academy of Sciences, Flemingovo nám. 2, Prague 16610, Czech Republic

**ABSTRACT:** Long-range ordering of water around solutes has been repeatedly invoked as the key to its biological function. Recently, it has been shown that in an 8 mM aqueous NaCl solution the orientational correlation between water molecules extends beyond 8 nm. This was interpreted as arising from ion-induced long-range effects on the water collective hydrogen-bond interactions. Each ion was suggested to affect >10 000 water molecules, leading to a picture involving nanoscopic “ordered domains”. Using molecular dynamics simulations, we show that the very small long-range tail in the correlation function is caused primarily by pairs of water molecules belonging to different ions’ hydration shells and can be made to practically disappear by rearranging the ionic positions. This means that the ion-induced water orientational ordering in millimolar salt solutions cannot be separated from ion–ion interaction effects, for which the Debye–Hückel screening length shrinks to less than 1 nm at physiological ionic strengths.



The Debye–Hückel screening length  $\lambda_D$  determines the range of mutual interactions of charged particles.<sup>1–3</sup> More specifically, for salt ions dissolved in water, the electric field decreases exponentially by a factor of  $1/e$  at a distance of  $\lambda_D = 0.304I^{-1/2}$  nm, where  $I$  is the ionic strength of the solution.<sup>1,2</sup> At physiological concentrations of  $\sim 150$  mM (which is, strictly speaking, beyond the quantitative validity of the Debye–Hückel theory), the screening length is about 0.8 nm, while in more dilute  $\sim 1$  mM solutions, it increases to almost 10 nm. This sensitive dependence of the electrostatic screening of salt ions on their concentration in water is one of the cornerstones of theories of electrolytes.<sup>3</sup>

Recently, a combined experimental and computational study suggested that in dilute aqueous salt solutions of about  $10 \mu\text{M}$  to a few mM, long-range water–water correlations induced by the ions can be observed.<sup>4</sup> Following the definition implicitly employed in ref 4, here we will use the term “long range” to designate ion-induced structural effects that extend beyond the first few hydration layers, that is, typically beyond 1 nm. Simulations of an 8 mM NaCl solution showed that a small angular correlation between pairs of water molecules persists up to distances of at least 8 nm (limited by the employed simulation unit cell size). The interpretation provided in ref 4, where the simulations were performed primarily to support the accompanying experimental observations, has been that each ion in dilute salt solutions induces nanoscopic “ordered domains” containing  $10^4$ – $10^6$  surrounding water molecules. This claim may, however, appear to be at odds with the very short distance at which water molecules become mutually uncorrelated in the aqueous bulk. Ion–ion interaction energies become smaller than the thermal energy for separations greater

than the Bjerrum length, which in room-temperature water amounts only to 0.7 nm.<sup>5</sup> Because water–ion and water–water correlations decay more rapidly than ion–ion interactions with increasing separation, in pure water, orientational correlations become effectively negligible beyond 1 nm.<sup>4</sup> In the rest of this Letter, we elaborate on this issue by means of molecular simulations. We specifically focus on the ion-induced long-range structural correlation between water molecules that was inferred from simulations in ref 4, while we do not address here the experimental results of ref 4. We provide a careful assessment of the size of the long-range water–water orientational correlations together with a refined interpretation thereof including the effects of ion–ion correlations within the extent of the Debye–Hückel screening length.

As a first step, we reproduced the simulation results from ref 4 concerning an 8 mM aqueous solution of NaCl. Figure 1 shows the resulting distance-weighted water–water orientational correlation function  $\langle \cos(\theta) \rangle R^2$  (black line), where  $\theta$  is the angle between the dipoles and  $R$  the distance between their respective oxygen atoms. Our results confirm that the previously reported long-range tail of the correlation function extending to distances  $R$  of almost 10 nm is real, albeit of a very small magnitude. It follows from basic electrostatics that orientational correlations of dipolar solvent molecules around an ion decay at longer distances as  $R^{-2}$ . Unlike the strong short-range (subnanometer) water–water orientational correlations, the long-range tail is thus only visible when distance-weighted,

Received: March 27, 2017

Accepted: April 21, 2017

Published: April 21, 2017

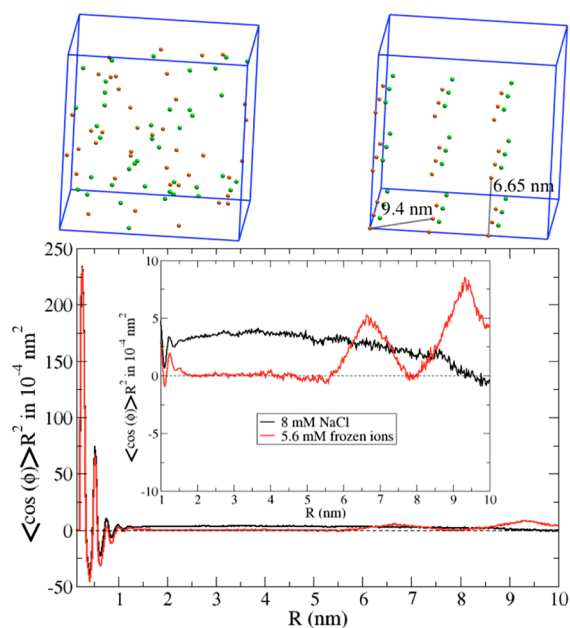


**Figure 1.** (Top) Snapshots of ionic arrangements in an unconstrained 8 mM NaCl solution (left) and in a 5.6 mM NaCl solution with a fixed regular arrangement of ions (right). (Bottom) Corresponding distance-weighted water–water orientational correlation functions (black and red lines). The inset zooms in the correlation for distances larger than 1 nm.

that is, multiplied by  $R^2$ , as already noted in ref 4. Even then, the values at the tail of the correlation function are less than  $5 \times 10^{-4} \text{ nm}^2$ . This value should be compared to the standard deviation of  $\cos(\theta)$  multiplied by  $R^2$ , which becomes many orders of magnitude larger than the distance-weighted water–water orientational correlations for distances beyond 1–2 nm (see Figure 2). Assuming for simplicity that this  $5 \times 10^{-4} \text{ nm}^2$  angular correlation at 4 nm arises from a harmonic potential of  $(1/2)k[\cos(\theta) - 1]^2$ , it is straightforward to show that the energy difference  $k$  between the parallel and antiparallel water dipole orientations is less than  $0.0001k_B T$ , which simply cannot lead to nanoscopic “ordered domains”<sup>4</sup> in water at ambient conditions.

What is the origin of the small long-range tail of the water–water orientational correlations in dilute salt solutions? To address this issue, we first consider the case of a single ion. Depending on the ion’s charge, the preferred orientation of a dipole moment of a water molecule is (anti-)parallel to the ion–water radial direction; the point charge–water dipole interaction decays as  $1/R^2$ , and the  $R^2$  distance weighting would lead to a constant distance-weighted correlation, independent of  $R$  (Figure 2). Beyond about 1 nm, the ion–water interaction is smaller than the thermal energy, but once the thermal fluctuations are averaged out, a small residual angular correlation persists, even though these water molecules do not form ordered domains. We now analyze dilute salt solutions and investigate which water molecules contribute to the water–water angular correlation. We first stress that while pairs of water molecules in the vicinity of the same ion exhibit the largest correlation, the  $R^2$  distance weighting puts the emphasis on pairs of water molecules that are much more weakly correlated but whose population is larger. The inset of Figure 2 clearly demonstrates that water molecules that are found around the same ion (i.e., for which the nearest ion is the

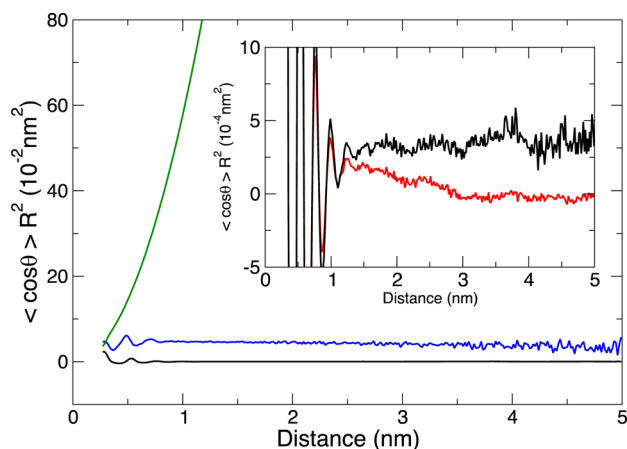


**Figure 2.** Comparison between the distance-weighted long-range water–water orientational correlations  $\langle \cos \theta \rangle R^2$  in an unconstrained 8 mM NaCl solution (black) and the corresponding distance-weighted standard deviation  $\sqrt{\langle [\cos \theta]^2 \rangle - \langle \cos \theta \rangle^2} R^2$  in green (which is very close to the isotropic limit of  $R^2 \sqrt{1/3}$ ). The blue curve depicts the angular correlation between the water dipole and the vector between the water oxygen and the nearest cation as a function of the ion–water distance, demonstrating how small this long-range orientational correlation, and even more so the long-range water–water orientational correlation, is compared to the standard deviation of the cosine of the corresponding angle. The inset shows again the distance-weighted long-range water–water orientational correlations (black) together with the contribution from water molecules around the same ion (red), which vanishes beyond 2 nm.

same) have a vanishing contribution beyond 2 nm. In other words, the long-range tail originates primarily from orientational correlations between pairs of water molecules whose nearest ions are different and that thus belong to different ion solvation shells (our analysis further shows that the largest contribution to the long-range correlation comes from pairs of water molecules both within 1–3 nm from their closest ions). This immediately brings the idea to try to influence the behavior of this tail by performing additional simulations at comparable salt concentrations, in which the positions of ions are initially arranged in various patterns and then kept fixed. One such ion arrangement is presented in Figure 1, which also shows the resulting water–water orientational correlation function (red line). While in these dilute solutions with average nearest-neighbor ion–ion distances of several nanometers the short-range (subnanometer) correlations were insensitive to the particular ionic arrangement, the long-range correlations were not. This is demonstrated in Figure 1, which shows that for the presented ionic arrangement the long-range tail of the correlation function practically vanishes up to about 5 nm. Moreover, the peaks at 6.65 and 9.4 nm match perfectly the chosen smallest and second smallest distances between like charge ions.

The above observations point directly to the fact that the long-range tail of the water–water orientational correlation function is strongly influenced by ion–ion correlations. In other words, the ions themselves are correlated and, therefore, also their hydration shells are orientationally correlated at the Debye–Hückel screening length, which extends in these dilute solutions to 5–10 nm. This is also why merely by rearranging the ions the long-range water–water orientational correlations can be completely changed (and even zeroed out for  $2 < R < 5$  nm); see Figure 1.

From the technical point of view, it is important to note that the exact shape of the long-range tail of the water–water orientational correlation function can depend sensitively on the boundary conditions chosen for the simulations. Indeed, Figure 3 demonstrates that in pure water the often utilized tin foil

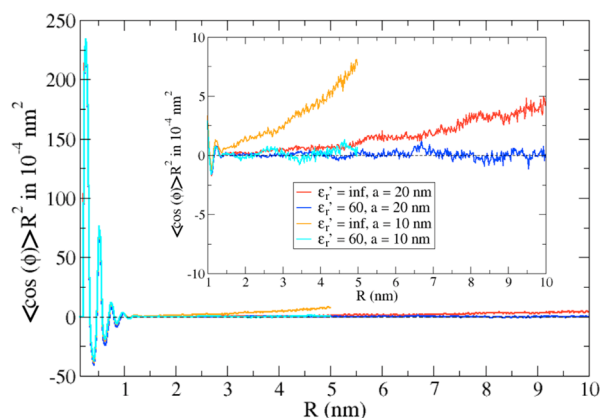


**Figure 3.** Distance-weighted water–water orientational correlation functions in neat water. Comparison of two types of Ewald boundary conditions: a tin foil  $\epsilon_r' = \infty$  (red) vs. 60 (blue) for two sizes of the unit cell of approximately 10 and 20 nm. The inset zooms in the correlation functions for distances larger than 1 nm.

Ewald boundary condition,<sup>4,6,7</sup> corresponding to a dielectric constant of  $\epsilon_r' = \infty$ , leads to a spurious increase of the distance-weighted water–water orientational correlations at large distances. This artifact decreases with increasing system size; nevertheless, it is still clearly present even for the largest employed 20 nm simulation cell. In fact, the size of this artifact in neat water is comparable to the effect of millimolar salt on the tail of the correlation function discussed above (Figure 1). For example, at distances of 5 nm or more, we found that the magnitude of the observed ion-induced correlation changes by more than a factor of 2 with the choice of boundary conditions, despite the large 20 nm dimension of the simulation box. The proper way to deal with this issue<sup>8</sup> is to set the value of the dielectric constant at the unit cell boundary to that corresponding to the simulated water model, that is, about 60.<sup>9</sup> We note that the artifacts due to the tin foil boundary condition tend to disappear as salt is added to the solution, changing it from an insulator to a conductor provided that a sufficiently large unit cell is employed.<sup>4</sup>

Our conclusion that the small long-range tail in the water–water orientational correlation function is strongly influenced by ion arrangements is further supported by its concentration dependence behavior. Figure 4 presents the results obtained from simulations with a unit cell size of 10 nm for four concentrations from 17 mM to 1 M, compared to neat water. While for shorter distances the correlation function increases with the amount of dissolved salt, at larger distances, it decays faster at higher concentration. For physiological concentrations, the distance-weighted orientational correlation function becomes negligible beyond  $\sim 2$  nm, while at 1 M, the electrostatic screening is such that the correlation function vanishes beyond 1 nm similarly as in neat water.

The importance of our present findings goes beyond an academic discussion about the proper interpretation of the small long-range tail of the water–water orientational correlation function in dilute salt solutions. The relevance of

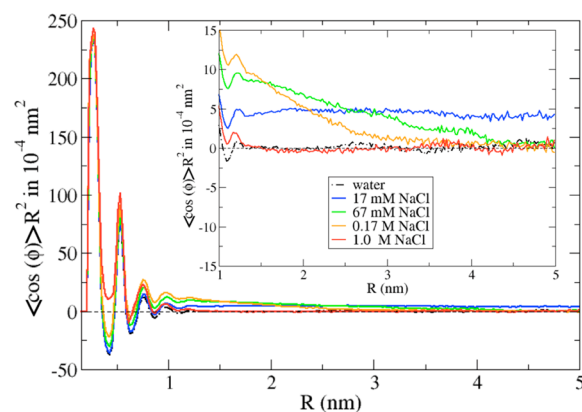


**Figure 4.** Concentration dependence of the distance-weighted water–water orientational correlation in a  $\sim 10$  nm simulation cell comparison of neat water (black dashed–dotted line) and solutions with different NaCl concentration (color solid lines). The inset zooms in the correlation for distances larger than 1 nm.

long-range effects in aqueous solutions has been widely debated, and it has been claimed, for example, that long-range “allosteric” effects in water could be a possible key to its biological function.<sup>10,11</sup> While ref 4 does not join such claims, its description involving tens of thousands or more water molecules organized around an ion and forming nanoscopic “ordered domains”<sup>4</sup> may be viewed as overreaching. Our present study shows that the small ion-induced structural correlation between water molecules can be explained within a more sober picture that does not support the notion of long-range effects in the role of water in biological environments. The influence of ions is only important for water molecules in their vicinity, and correlations between water molecules are of a local character. The small long-range tail in the correlation function is due to correlations between water molecules belonging to solvent shells of different ions, and by simply rearranging the ionic positions, it can be effectively attenuated. This tail thus strongly depends on ion–ion correlations, the extent of which is given by the Debye–Hückel screening length. This length is on the order of 10 nm in millimolar salt solutions but shortens to less than 1 nm at a physiological ionic strength. Our findings reinforce the notion of water as a solvent that responds to solute molecules locally, leaving potential long-range allosteric effects to the solutes themselves.

## ■ COMPUTATIONAL METHODS

First, we performed molecular dynamics simulations for the same diluted aqueous salt solution as in ref 4. Namely, the simulated system consisted of 264363 TIP4P/2005 water molecules<sup>12</sup> with 40  $\text{Na}^+$  and 40  $\text{Cl}^-$  ions described by the CHARMM36 force field.<sup>13</sup> We have shown in our previous study that such a nonpolarizable force field performs satisfactorily for this system, where effects of electronic polarization are modest.<sup>14</sup> The geometry of water molecules was kept rigid by the SETTLE algorithm. The equations of motion were integrated using the leapfrog algorithm with a time step of 2 fs using the Gromacs 4.6.5 software.<sup>15</sup> Three-dimensional periodic boundary conditions were applied. Short-range electrostatic and van der Waals interactions were truncated at 0.9 nm, with the long-range electrostatic interactions being accounted for via the smooth particle mesh Ewald method with a grid spacing of 0.12 nm employing tin foil Ewald boundary conditions.<sup>16</sup> We collected ten 5 ns trajectories

(50 ns in total) in an *NVT* ensemble at a temperature of 298 K maintained by the canonical velocity rescaling thermostat<sup>17</sup> with a coupling constant of 1 ps. The total simulation length was sufficient to converge the water–water orientational correlation function, which was sampled every 2 ps.

Initial configurations were taken from a 2 ns equilibration at a constant pressure of 1 bar using the Berendsen barostat<sup>18</sup> with a coupling constant of 0.5 ps and at a constant temperature of 298 K using the canonical velocity rescaling thermostat<sup>17</sup> with a coupling constant of 0.1 ps. The initial configurations were then obtained from the last 450 ps with a time separation of 50 ps. The cell length was adjusted to 19.94 nm, and new velocities were generated.

To address the issue of the influence of ionic arrangement, we alternatively placed ions on a grid and kept their positions fixed. The 27 Na<sup>+</sup> ions were placed at ( $i \times a/3, j \times a/3, k \times a/3$ ), where  $i, j,$  and  $k = 0, 1,$  and  $2$  and  $a$  is the unit cell length. The interionic arrangement of Cl<sup>-</sup> is the same as that of Na<sup>+</sup>. The anionic grid is shifted with respect to the cationic one by 1.0 nm in all three directions, as is illustrated in Figure 1. The ionic grid was solvated by 264389 water molecules, and the unit cell length was adjusted to 19.94 nm. This was followed by a 600 ps equilibration in an *NVT* ensemble out of which the last 450 ps were used to generate initial configurations for the ten 5 ns production trajectories.

To check the influence of Ewald boundary conditions<sup>16</sup> on the water–water orientational correlation at large distances, we performed additional simulations for neat water with two types of Ewald boundary conditions: tin foil ( $\epsilon_r' = \infty$ ) and  $\epsilon_r' = 60$ . For 264443 water molecules in a 19.94 nm simulation cell, we applied the same computational protocol as that for the diluted salt solution, and we collected total of 50 ns of trajectories in total for each of the two boundary conditions.

To examine the system size dependence, we simulated pure water in a cell with half of the previous length. The system contained 33049 water molecules, and the production run cell length of 9.972 nm was determined from an average cell length over the 2 ns equilibration in the *NpT* ensemble. The last 200 ps of the equilibration provided five initial configurations for subsequent 20 ns production runs in the *NVT* ensemble for every configuration. The overall length of the simulation for both types of Ewald boundary conditions was thus 100 ns.

Finally, we also investigated the concentration dependence of the water–water orientational correlation function in a  $\sim 10$  nm unit cell. Each of the systems was at first equilibrated for 2 ns in the *NpT* ensemble, the average cell length from this equilibration providing the respective value for the subsequent production run in the *NVT* ensemble. We collected five 20 ns trajectories with tin foil boundary conditions for each of the investigated concentrations of 17 mM (10 Na<sup>+</sup> and 10 Cl<sup>-</sup>), 67 mM (40 Na<sup>+</sup> and 40 Cl<sup>-</sup>), 0.17 M (100 Na<sup>+</sup> and 100 Cl<sup>-</sup>), and 1.0 M (600 Na<sup>+</sup> and 600 Cl<sup>-</sup>).

## AUTHOR INFORMATION

### Corresponding Authors

\*E-mail: [eva.pluharova@jh-inst.cas.cz](mailto:eva.pluharova@jh-inst.cas.cz) (E.P.).

\*E-mail: [damien.laage@ens.fr](mailto:damien.laage@ens.fr) (D.L.).

\*E-mail: [pavel.jungwirth@uochb.cas.cz](mailto:pavel.jungwirth@uochb.cas.cz) (P.J.).

### ORCID

Damien Laage: 0000-0001-5706-9939

Pavel Jungwirth: 0000-0002-6892-3288

## Notes

The authors declare no competing financial interest.

## ACKNOWLEDGMENTS

E.P. thanks the Czech Science Foundation (Grant No. 17-01982Y) and the Czech Academy of Sciences for the Postdoctoral Fellowship (Grant No. L200401651). P.J. acknowledges support from the Czech Science Foundation (Grant No. P208/12/G016). The research leading to these results received funding from the European Research Council under the European Union's Seventh Framework Program (FP7/2007-2013)/ERC Grant Agreement No. 279977 (DL).

## REFERENCES

- (1) Evans, D. F.; Wennerstrom, H. *The Colloidal Domain: Where Physics, Chemistry, Biology, and Technology Meet*; Wiley, 1999.
- (2) Israelachvili, J. *Intermolecular and Surface Forces*; Academic Press Inc., 1985.
- (3) Barthel, J. M. G.; Krienke, H.; Kunz, W. *Physical Chemistry of Electrolyte Solutions: Modern Aspects*; Springer, 1998.
- (4) Chen, Y. X.; Okur, H. I.; Gomopoulos, N.; Macias-Romero, C.; Cremer, P. S.; Petersen, P. B.; Tocci, G.; Wilkins, D. M.; Liang, C. W.; Ceriotti, M.; Roke, S. Electrolytes Induce Long-Range Orientational Order and Free Energy Changes in the H-bond Network of Bulk Water. *Sci. Adv.* **2016**, *2*, e1501891.
- (5) Curtis, R. A.; Lue, L. Depletion forces due to image charges near dielectric discontinuities. *Curr. Opin. Colloid Interface Sci.* **2015**, *20*, 19–23.
- (6) Levrel, L.; Maggs, A. C. Boundary conditions in local electrostatics algorithms. *J. Chem. Phys.* **2008**, *128*, 214103.
- (7) Kolafa, J.; Viererblova, L. Static Dielectric Constant from Simulations Revisited: Fluctuations or External Field? *J. Chem. Theory Comput.* **2014**, *10*, 1468–1476.
- (8) Boresch, S.; Steinhauser, O. Presumed versus real artifacts of the Ewald summation technique: The importance of dielectric boundary conditions. *Ber. Bunsen-Gesellschaft - Phys. Chem. Chem. Phys.* **1997**, *101*, 1019–1029.
- (9) Vega, C.; Abascal, J. L. F. Simulating water with rigid non-polarizable models: a general perspective. *Phys. Chem. Chem. Phys.* **2011**, *13*, 19663–19688.
- (10) Bagchi, B. *Water in Biological and Chemical Processes: From Structure and Dynamics to Function*; Cambridge University Press: Cambridge, U.K., 2013; pp 81–96.
- (11) Lynden-Bell, R.; Moris, S. C.; Barrow, J. D.; Finney, J. L.; Harper, C. L., Jr. *Water and Life: The Unique Properties of H<sub>2</sub>O*; CRC Press: Boca Raton, FL, 2010.
- (12) Abascal, J. L. F.; Vega, C. A general purpose model for the condensed phases of water: TIP4P/2005. *J. Chem. Phys.* **2005**, *123*, 234505.
- (13) Best, R. B.; Zhu, X.; Shim, J.; Lopes, P. E. M.; Mittal, J.; Feig, M.; MacKerell, A. D. Optimization of the Additive CHARMM All-Atom Protein Force Field Targeting Improved Sampling of the Backbone phi, psi and Side-Chain chi(1) and chi(2) Dihedral Angles. *J. Chem. Theory Comput.* **2012**, *8*, 3257–3273.
- (14) Kohagen, M.; Mason, P. E.; Jungwirth, P. Accounting for Electronic Polarization Effects in Aqueous Sodium Chloride via Molecular Dynamics Aided by Neutron Scattering. *J. Phys. Chem. B* **2016**, *120*, 1454–1460.
- (15) Hess, B.; Kutzner, C.; van der Spoel, D.; Lindahl, E. GROMACS 4: Algorithms for highly efficient, load-balanced, and scalable molecular simulation. *J. Chem. Theory Comput.* **2008**, *4*, 435–447.
- (16) Essmann, U.; Perera, L.; Berkowitz, M. L.; Darden, T.; Lee, H.; Pedersen, L. G. A Smooth Particle Mesh Ewald Method. *J. Chem. Phys.* **1995**, *103*, 8577–8593.
- (17) Bussi, G.; Donadio, D.; Parrinello, M. Canonical sampling through velocity rescaling. *J. Chem. Phys.* **2007**, *126*, 014101.

(18) Berendsen, H. J. C.; Postma, J. P. M.; Vangunsteren, W. F.; Dinola, A.; Haak, J. R. Molecular-Dynamics with Coupling to an External Bath. *J. Chem. Phys.* **1984**, *81*, 3684–3690.